RECONSTITUTING FUNDAMENTALS OF BACTERIA MEDIATED CANCER THERAPY ON A CHIP

Wonjun lee[1], Jiin Park[2], Dongil Kang[3] and Seungbeum Suh[4]*
[1]Department of Mechanical Engineering, Seoul National University, Republic of Korea
[2]Department of Life Science, Ehwa Womans University, Republic of Korea
[3]Department of Biomedical Engineering, Hanyang University, Republic of Korea
[4]Center for Healthcare Robotics, Korea Institute of Science & Technology, Republic of Korea

ABSTRACT

This paper reports a microfluidic platform tailored for emulating fundamentals of bacteria-mediated cancer therapy (BMCT). Specifically, we attempted to replicate the basic features of the bacteria-colonized tumor microenvironment and the accompanying immune response in a single well of the device. The effects of bacterial stimulation on tumor spheroids were observed to experimentally examine bacteria's innate antitumor cytotoxicity and potential as a therapeutic agent carrier *in vitro*. Consequently, we observed enhanced dead signals as well as decreased stemness of tumor spheroids as a result of bacterial cytotoxicity and IFN- β secretion, respectively. Furthermore, enzyme-linked immunosorbent assay results from cell culture media indicative of co-cultured macrophage's M1 polarization demonstrated bacteria's potential for immune-activating adjuvant. Our device, with a user-friendly platform leveraging spontaneous capillary, will offer a chance to scrutinize BMCT at cellular and tissue levels.

KEYWORDS

Organ-on-a-chip, Bacteria mediated cancer therapy, Tumor microenvironment

INTRODUCTION

In recent years, technical advances in the biomedical area have dramatically augmented our understanding of oncology, and this body of knowledge has been successfully translated into novel treatments or strategies for cancer. However, the hypoxic environment of the tumor microenvironment (TME) still remains to be a major hurdle for researchers since it not only restricts therapeutic efficacy but also directly promotes the establishment of a tumor immunosuppressive milieu [1]. The workaround adopted by some researchers was to utilize hypoxia-responsive nanoparticles to achieve a preferential engagement in hypoxic tumor tissues, but the inactive nature of nanoparticles resulted in unsatisfactory outcomes [2]. In this context, the hypoxia-targeting capacity of bacteria has drawn attention to using bacteria as an effective therapeutic agent in cancer therapy. In addition to hypoxia targeting ability, their immunogenicity produced a positive antitumor immune response, further breaking new ground for bacteria-based tumor immunotherapy [3]. The complexity of bacteria as living organisms was ambivalent to researchers. Achievement of unprecedented antitumor action was possible with fine-tuning of many functionalities, though challenging.

However, due to the intricacy of the triangular interactions between bacteria, tumors, and the immune system, contemporary works on BMCT are mostly academic rather than practical and limited to engineered model organisms. Their method of examining resected tumors or mice inoculated with bacteria and cancer precludes the analysis of intrinsic features of individual cells underlying the phenomenon. Furthermore, given the substantial disparities in fundamental physiology between humans and engineered model organisms, it is evident that such restrictions might lead to translational failure and impede future "bench-to-bedside" BMCT deployment. Therefore, a more human-centric *in vitro* solution to support current *in vivo* models for their use as “pre-preclinical” assessments of BMCT is in demand.

To this end, we propose a novel microfluidic platform optimized using a rapid prototyping technique to recapitulate the fundamentals of BMCT *in vitro*. Here, we aimed to emulate the basics of 1) a bacteria-colonized tumor microenvironment and 2) the corresponding immune response in a single well of the microfluidic device. Macrophages and bacteria-stimulated tumor spheroids were selectively patterned into defined regions of the device by spontaneous capillary flow under hydrophilic conditions. Increased pro-inflammatory cytokine production from macrophages indicated the implementation of the bacterial inflammation concept as patterned cells proliferated and generated a corresponding 3D tissue environment. As a disclaimer, let us emphasize that even though the assays we've done here were straightforward, our methodology is easily extensible for advanced systems that are more sophisticated.

MATERIALS AND METHODS

Platform design and fabrication

The PMMA chip body of the microfluidic device was fabricated by a commercial CO2 laser cutter (Epilog Mini 24, Epilog). The inlets and open-channel reservoirs were created with vector cut, whereas the microchannels were created by raster engraving mode. According to the desired microchannel dimensions, the laser’s speed and power were mutually adjusted (Figure 1B). Solidworks (Dassault System, USA) was used to transfer drawings to the laser cutter. 3M™ 9795R advanced polyolefin diagnostic microfluidic medical tape (thickness: 50 μm) as the substrate for the chip was then subsequently bonded to the UV sterilized PMMA body part to complete the device.

Bacterial strains and materials

The microbial species used are *Escherichia coli* (*E. coli*), *Salmonella Typhimurium* (*S. typhimurium*), and IFN-

β secreting *S. typhimurium* (kindly provided by Dr. Heung Jin Jeon, Chungbuk National University). The microbial species were cultured overnight at 37°C in a Luria-Bertani (LB) broth under shaking conditions. 100 µL overnight cultures were inoculated in 10 mL fresh LB broth and incubated at 37 °C and 100 rpm in the shaking incubator. Once the bacteria were confirmed to be in the log phase (OD600 at 1.2), cells were collected by centrifugation at 6000 rpm for 5 min. After discarding the supernatant, the bacterial pellet was suspended in 1x phosphate-buffered saline (PBS; Gibco), and the concentrations were properly adjusted according to the experimental requirements.

Cell cultivation and spheroid preparation

Human umbilical endothelial cells (HUVECs; Cefobio, Korea) were cultured in endothelial growth medium 2 (EGM-2; Lonza) and used in experiments between passages 4-5. NIH-3T3 (KCLB, Korea) cell line and macrophages RAW 264.7 (KCLB, Korea) were cultured in Dulbecco's modified Eagle's medium (DMEM; Hyclone) supplemented with 10% fetal bovine serum (FBS; HyClone, USA) and 1% penicillin-streptomycin (PS; Gibco, USA). The murine breast cancer cell line 4T1 (ATCC, USA) was cultured in Roswell Park Memorial Institute 1640 (RPMI; Hyclone) supplemented with 10% FBS and 1% PS. All cells were maintained in a humidified incubator at 37°C and 5% CO2.

Cell suspensions were harvested in a 1% agarose (Promega, USA) pre-coated 96-well plate with a U-shaped bottom well (SPL Lifescience, Korea) to prepare spheroids for the experiments. Co-culture tumor spheroids were initiated by mixing 4T1s and NIH-3T3s (at a ratio of 2:1; total cell was 15,000). After pre-culturing in a wellplate for 4–5 days, spheroids were stimulated with different bacterial agents before the experiment. After stimulation, spheroids were washed with 1× PBS gently and treated with 100 µg/mL gentamicin for 2 h to kill extracellular bacteria.

Hydrogel and cell patterning

Prior to loading, the surface of the microfluidic device was hydrophilized with plasma surface treatment at 70W for 3 min (Femto Science, Korea). The following steps were taken to pattern the cells in the chip: the central channel was patterned with 9 µL of cellular (RAW 264.7, final concentration 1×10^6 mL^{-1}) Matrigel solution (final concentration 2.5 $mgmL^{-1}$; Corning, USA). Stimulated spheroid and control spheroid were encapsulated into cellular Matrigel solution (NIH-3T3, final concentration 1×10^6 mL^{-1} & HUVECs, final concentration 3×10^6 mL^{-1}) and were then introduced to the upper side channel and lower side channel, respectively. After waiting 45 min for the gels to polymerize, EGM-2 was added to the reservoirs, and the chips were kept in an incubator.

RESULTS AND DISCUSSION

Design and function of Microfluidic device

The microfluidic device used in this study consists of single PMMA body housing the microfluidic patterning geometries and the media reservoir, with an adhesive bonded to a polycarbonate (PC) film substrate. Each unit well consists of 3 microchannels that are disposed in

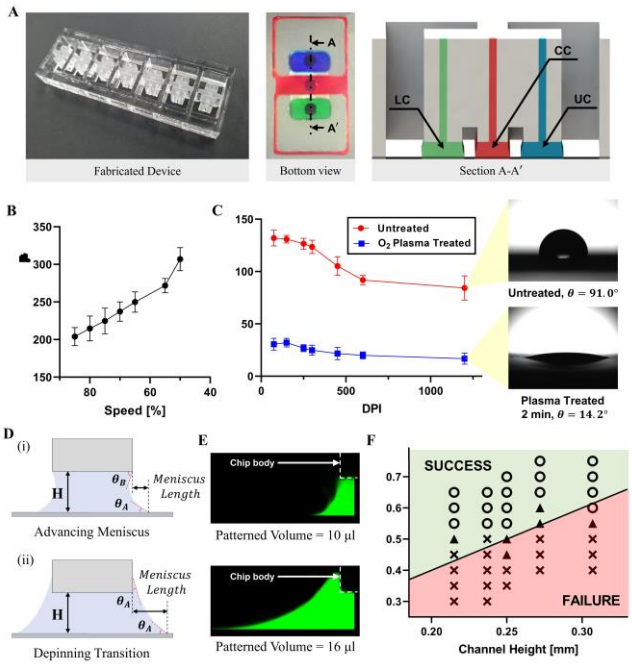

Figure 1: A) Representative images and conceptual rendering of the fabricated microfluidic device. B) Laser engraved depth of PMMA with different laser speeds. C) The results of contact angle measurements before and after plasma treatment on engraved PMMA with different DPI. D) Schematic illustration of two possible capillary liquid configurations. E) Images of the cross-sections of the devices filled with a FITC solution under the noted volume. F) Design criteria for optimal fluid patterning between distinct channels in terms of volume and distance.

parallel and partitioned along perpendicular distances (Figure 1A). Working as a pathway of nutrition and oxygen, all three channels are directly exposed to the media chamber for cell feeding. The cell patterning region contains a single hole in the center, designed to capture a large spheroid. Liquid can be patterned in the designated structure by directly sticking a pipette into the injection hole. Contrary to the central channel (CC), the upper channel (UC) and lower channel (LC) allow for spatial separation of the patterned cells since the liquid is injected directly into it without passing through a wedge or other injection port. Compared to equivalent conventional soft lithographic PDMS-based platforms, our laser-cutter-manufactured platform is capable of much higher throughput and flexibility in terms of operation and fabrication [4]. In contrast to soft lithography, which takes multiple steps, this rapid prototyping requires only one: transferring a prepared file to the laser cutter and then waiting for the output. This simplicity has the consequence of increasing design flexibility, which adds to the convenience of optimization. The primary issue with PDMS-based devices, small molecule adsorption, is also resolved by the material choice of a PMMA body and a silicon-based substrate [5]. The aforementioned traits all together made it easier to optimize the microfluidic device and deploy a 3D culture for emulating a bacteria-colonized tumor microenvironment (TME).

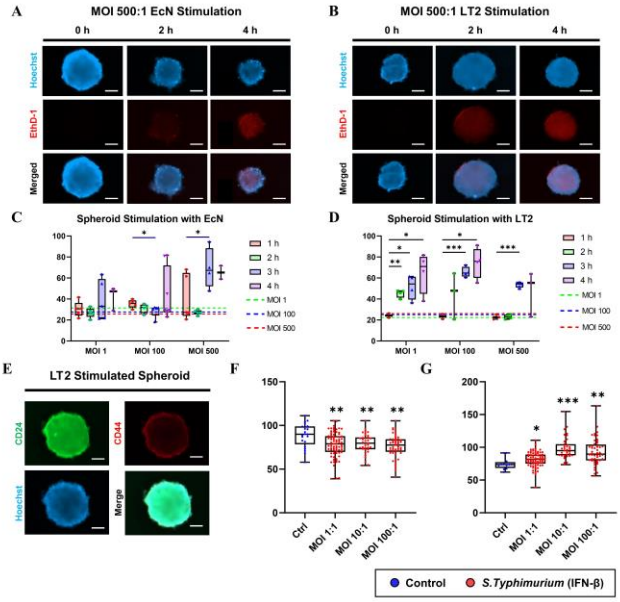

*Figure 2: A-B) Representative images of co-culture tumor spheroid (4T1 and NIH3T3) stained with ethidium homodimer-1 (red; dead cells) and Hoechst (blue; nuclei) in the presence of bacterial inflammation of Escherichia coli (E.coli) and S.typhimurium, respectively. Scale bars, 100 μm. C-D) Box plot of normalized fluorescent intensity of ethidium homodimer-1 from the E.coli and S.typhimurium inflammation model, respectively. E) Representative images of tumor spheroids stained with Hoechst (blue), CD24 (green), and CD44 (red) from the S.typhimurium (IFN-β) inflammation model. Scale bars, 100 μm. F-G) Normalized intensities of CD24 and CD44 expression in tumor spheroids from the S.typhimurium (IFN-beta) inflammation model after 18 h of infection under different MOI. *p < 0.05, **p < 0.005, and ***p < 0.0005 in two-tailed unpaired t-tests.*

Selective Microfluidic Patterning

The designed microfluidic device utilizes air plasma-induced hydrophilic surface modification to facilitate spontaneous capillary flow patterning (SCP) of droplets [6] (Figure 1-C). In essence, liquid confined in a slit of hydrophilic surface does not maintain a right-angled air-liquid contact, which might result in the failure of hydrogel patterning. The capillary liquid underneath the body will initially form a concave interface when loaded along the injection port and advance toward the structure's perimeter while maintaining θ_A as a contact angle with the bottom substrate. Since the bottom substrate is large enough, the menisci meet it at Young's contact angle θ_A, but there are two alternatives for each menisci's top portion: (1) They may be pinned at the edges, forming an angle of θ_B w.r.t. the horizontal, and (2) the menisci may be unpinned and placed outside the open ends, with the contact angle θ_A wetting sidewall of the rail [7] (Figure 1D). The air-liquid meniscus length on the bottom substrate must be meticulously managed under these circumstances in order for the liquid in each channel to be precisely patterned without interfering with one another, making instance (1) more conducive to patterning [8]. Accordingly, the proper liquid volume was estimated under the assumption that the menisci were circumferential and that their surfaces were entirely hydrophilic ($\theta_A = 0$, $\theta_B = \pi/2$). Half of the distance between the two channels must be less than the meniscus length for the channel to be selectively patterned, and meniscus length L can be formulated as follows:

$$\mathbf{L} = \mathbf{H_0} tan\left(\frac{\theta_B}{2} - \frac{\theta_A}{2}\right) < \mathbf{H_0} \qquad (1)$$

where θ_A, θ_B, and H_0 are the bottom contact angle, body contact angle, and channel height, respectively. A parametric study was conducted to validate this theoretical analysis. Different channel heights and spacing were used during the experiment. A designated volume of PBS was injected into each channel, which was then examined to see if any coloring mixture had happened. The correctness of the theoretical analysis was validated in the majority of experimental groups and corroborated the design rule for successful patterning (Figure 1F). We hypothesize that the laser cutter's instability is to blame for minor failures that occur close to the boundary.

Bacterial stimulation on tumor spheroid

One of the primary advantages of using bacteria for cancer treatment is their ability to target tumors and colonize them preferentially. In this respect, the intrinsic antitumor cytotoxicity of bacteria produced synergistic outcomes with endeavors to design bacteria as a producer

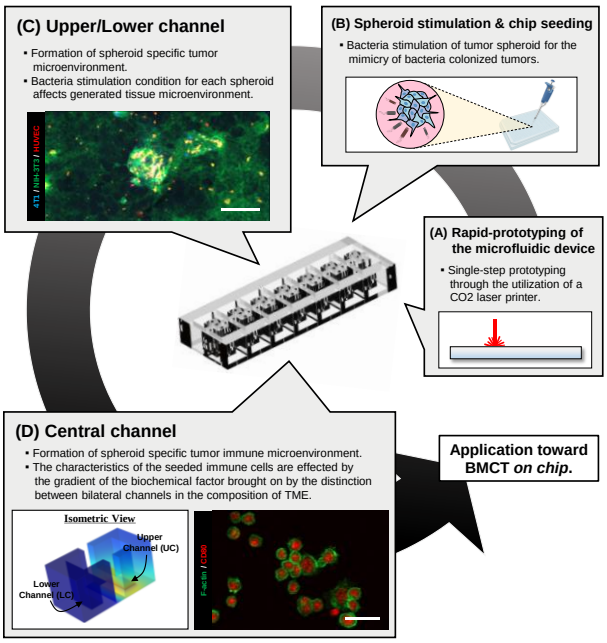

Figure 3: The overall experiment schematic for on-chip generation of bacteria-colonized TME. A) The fabricated device was cut and assembled in minutes through rapid prototyping. B) A conceptual illustration of the spheroid stimulation process. C) Representative confocal image of generated TME stimulated with S.typhimurium. Scale bar = 500 μm. D) Computational simulation showing the effect of the source configured in the upper channel to the lower channel through concentration gradients. Representative confocal image of RAW264.7 showing pro-inflammatory polarization after 4 days of coculture. Scale bar = 25 μm.

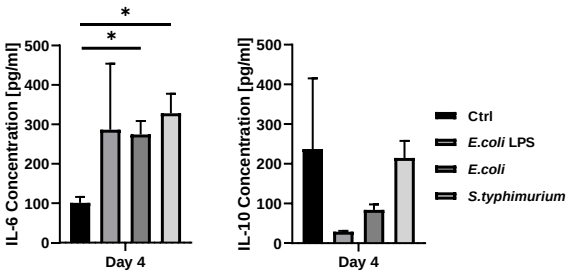

*Figure 4: ELISA results from cell culture media after 4 days of co-culture. The secretion of pro-inflammatory cytokines was greater in RAW264.7 cells cocultured with tumor spheroids stimulated by bacterial agents (E.coli, S.typhimurium, E.coli lipopolysaccharide). Bars indicate mean ±SEM. *p < 0.05, **p < 0.005, and ***p < 0.0005 in two-tailed unpaired t-tests.*

of nanomaterials or immunotherapeutic molecules by genetic engineering, thus forging new ground for the cancer immunotherapy paradigm. To verify this notion, the antitumor cytotoxicity of bacteria was first observed with tumor spheroid stimulation (Figure 2A). The proportion of dead cells grew with time in both *E.coli* and *S.typhimurium* infections, and the trend was clearly more prominent in the more virulent *S.typhimurium* infection (Figure 2D). Furthermore, when *S.typhimurium* was genetically engineered to secrete IFN-β, it not only reduced tumor survival rate but also successfully repressed cancer stem cell properties (Figure 2F). This observation is consistent with previous studies demonstrating positive clinical outcomes for the therapeutic usage of IFN-β in treating drug-resistant, highly aggressive triple-negative breast cancer [9]. The biological properties of the spheroid prepared through this method mirror the chemical properties of the used bacterial stimulant, i.e., toxicity, strain characteristic, and designed secreting factor. When transferred to the chip, these stimulated spheroids retain the key features of bacteria-cancer interaction and thus contribute to the generation of bacteria-colonized TME *in vitro*.

Reconstituting bacteria colonized TME

Figure 3 depicts a schematic representation of the experimental procedure using our apparatus. As a proof of concept, RAW 264.7 cells were seeded in the CC with *S. typhimurium*-stimulated tumor spheroid in the UC and control spheroid without any stimulation in the LC. Seeded cells proliferated and created a corresponding 3D tissue environment after 4 days of co-culture, contributing to the development of multifunctional TME on-chip (Figure 3C).

Enzyme-linked immunosorbent assay (ELISA) was conducted to confirm whether the concept of the bacterial inflammation model was successfully implemented in the device. As a result, we were able to establish that the bacterial treatment of tumor spheroids elicited an activated immune response in the microfluidic device since RAW 264.7 cells secreted more pro-inflammatory cytokines when co-cultured with bacteria-stimulated tumor spheroids (Figure 4). Promoted pro-inflammatory M1 polarization of macrophages indicates that the designed device can emulate the basic immunostimulatory mechanism of BMCT.

CONCLUSION

In this research, we presented a microfluidic platform that can mimic the fundamental pathophysiology of BMCT. The design rules for precise liquid patterning and reproduced salient features of bacteria colonized TME utilizing bacteria-stimulated tumor spheroid ensured successful *in vitro* reconstruction of tumor microbe microenvironment. The proposed methodology is of generic impact and easily transposable to more advanced systems with different cell culture approach. We envision that our strategy will expand existing research on BMCT that has been restricted to the traditional mouse model, thereby bridging laboratory and clinical practice.

REFERENCES

[1] M. Binnewies, et al. “Understanding the tumor immune microenvironment (TIME) for effective therapy”, *Nature medicine*, vol. 24, pp. 541-550, 2018.

[2] X. Huang, et al. “Hypoxia-tropic protein nanocages for modulation of tumor-and chemotherapy-associated hypoxia.”, *Acs nano*, vol. 13, pp. 236-247, 2018.

[3] X. Huang, et al. “Bacteria-based cancer immunotherapy”, *Advanced Science*, vol. 8, 2003572, 2021.

[4] A. E Ongaroa, N. Howartha, V. La Carrubbac, M. Kersaudy-Kerhoas, “Rapid prototyping for micro-ngineering and microfluidic applications”, *Advances in Manufacturing Technology XXXII*, vol. 8, pp. 107-112, 2018.

[5] M. W Toepke, D. J Beebe, “PDMS absorption of small molecules and consequences in microfluidic applications”, *Lab on a Chip*, vol. 6, pp. 1484-1486, 2006.

[6] S. B Berry, et al. “Upgrading well plates using open microfluidic patterning”, *Lab on a Chip*, vol. 17, pp. 4253-4264, 2017.

[7] A. Malijevsky, A. O Parry, “Edge contact angle, ` capillary condensation, and meniscus depinning”, *Physical Review Letters*, vol. 127, 115703, 2021.

[8] S. Kim, et al. “Anchor-impact: A standardized microfluidic platform for high-throughput antiangiogenic drug screening”, *Biotechnology and Bioengineering*, vol. 118, pp. 2524-2535, 2021.

[9] C. Fillmore, C. Kuperwasser, “Human breast cancer stem cell markers cd44 and cd24: enriching for cells with functional properties in mice or in man?”, *Breast cancer research*, vol. 9, pp. 1-3, 2007.

[10] M. R Doherty, et al. “Interferon-beta represses cancer stem cell properties in triple-negative breast cancer”, *Proceedings of the National Academy of Sciences*, vol. 114, pp. 13792-13797, 2017.

CONTACT

*S. Suh. Public, tel: +82-9427-8195;
keenhurt81@kist.re.kr